



OPEN ACCESS

EDITED BY

Jaroslav Rybak,
Wrocław University of Science and
Technology, Poland

REVIEWED BY

Providence Habumuremyi,
Fuzhou University, China
Beata Nienartowicz,
Warsaw University of Technology, Poland

*CORRESPONDENCE

Aslam Abdullah M,
✉ aslamabdullah.m@vit.ac.in

RECEIVED 15 December 2025

REVISED 04 February 2026

ACCEPTED 10 February 2026

PUBLISHED 26 March 2026

CITATION

R H and M AA (2026) Multifactorial analysis
of drill pipe failure in horizontal directional
drilling: a review.

Front. Built Environ. 12:1767777.

doi: 10.3389/fbuil.2026.1767777

COPYRIGHT

© 2026 R and M. This is an open-access
article distributed under the terms of the
[Creative Commons Attribution License
\(CC BY\)](https://creativecommons.org/licenses/by/4.0/). The use, distribution or
reproduction in other forums is permitted,
provided the original author(s) and the
copyright owner(s) are credited and that
the original publication in this journal is
cited, in accordance with accepted
academic practice. No use, distribution or
reproduction is permitted which does not
comply with these terms.

Multifactorial analysis of drill pipe failure in horizontal directional drilling: a review

Harishwaran R and Aslam Abdullah M*

School of Chemical Engineering, Vellore Institute of Technology, Vellore, Tamil Nadu, India

Drill pipe failure during horizontal directional drilling is a common occurrence nowadays. Drill pipe, a common tool in the drilling process, plays an important role in the uninterrupted production and supply of oil and gas. Drill pipes are subjected to various types of loads and operate under diverse environmental conditions. The drill pipe failure is caused by decarburization, washout, grain boundaries, fatigue, bending moment, fracture, piercing, galling, axial forces, torque, torsional vibration, axial vibration, wear, and corrosion. These conditions can occur individually or in combination as a consequence of reducing the lifespan of drill pipe. The paper aims to examine the reasons for drill pipe failure and the methodology adopted to explore the same. Different aspects of each factor have been studied and discussed. This review leads to the conclusion that the failure is due to twelve major factors, and recommendations have been made to analyze them, depending on the type of failure.

KEYWORDS

corrosion, drill pipe failure, fatigue, horizontal directional drilling, wear

1 Introduction

During oil and gas exploration and development, drill pipe is subjected to bending, torsion, complicated alternate pulling, pushing, vibrating, bending, twisting, and extra loads in three dimensions, in addition to corrosion, wear, and fatigue, resulting in accidents during horizontal directional drilling (HDD) (Yonggang et al., 2011; Li et al., 2011; 2013). The efficacy of drilling and the safety of output are greatly impacted by the drill pipe's reliance (Cao, 2011).

The HDD method requires a suitable linear area to accommodate all the drilling equipment (Cocciolo and Zeleny, 2004). The HDD is the most effective technique from the perspective of cost and seismic risk mitigation. The pipelines of oil and gas crossing rivers, canals, motorways, railroads, and other unsuitable shallow buried locations are carried out using trenchless technology (Zhu, 2016). The HDD technology has advanced significantly in the recent past concerning trenchless laying of pipelines. The drill string/stem and rig are slanted during the buckling phase of HDD. Most drill stem components are horizontal and are under intense axial pressure throughout the process of HDD (Li et al., 2013). This technology not only drives down prices but also improves work efficiency, reduces environmental impact, and reduces project costs. HDD uses a reamer, which is a cutting instrument placed in front of a pipe string to create a tunnel. By rotating reamers of increasing diameter, the tunnel is excavated and gradually widened. Failure analysis is crucial for preventing or reducing repeated failure incidents (Li et al., 2011). To optimize the drill pipe structure design and lessen the impact of drill pipe fatigue on drilling, it is essential to understand that the failure due to fatigue of drill pipes employed in HDD (Cao, 2011).

Cutting tools and drilling fluid (also known as mud), which runs under high pressure through directional nozzles, are used to segregate soil particles. HDD in urban soil must

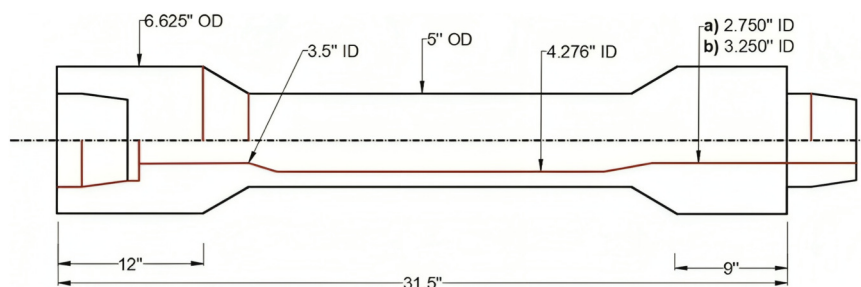


FIGURE 1 Illustration of drill pipe (dimension shown in inches).

meet the required minimum horizontal and vertical tolerances with existing features to limit the risk of damaging existing infrastructure (Booman et al., 2013). The upthrust created when the pipe is inundated with the drilling fluid during the HDD often pushes the pipe against the borehole walls. The weight and size of the pipe, the mud’s density, and the borehole’s form affect the normal contact force.

The contact force exerted normally in the curved sections of the bore pathway is significantly influenced by the curvature of the path, the bending stiffness of the pipe, and the applied pulling force (Chehab and Moore, 2010). Drill pipes are of two grades, S-135 and G-105, denoted as a and b in Figure 1. Figure 1 depicts the Illustration of a drill pipe. The Detailed Characteristics of Drill pipes and Tool joints of the two grades are listed in Tables 1, 2, respectively. It is discussed based on the material and mechanical characteristics of the drill pipe.

Statistics show that around 80% of drill pipe accidents during HDD were caused by drill pipe fatigue, mostly owing to fracture in the joint-thread and welding-line, galling of drill pipe’s screw thread, washout, piercing, and fracture, etc (Li et al., 2011; Cao, 2011; Cao et al., 2009; Fangpo et al., 2011). However, very few research has been done on the design of logical and analytical methods for the pipe, soil behavior, and drilling fluids during HDD installations (Polak and Lasheen, 2001). The failures in drill pipes during Horizontal directional drilling have been studied in this paper, with a particular focus on analyzing the failures. The summary of studies on the failure of drill pipes during HDD is given in Table 3.

Horizontal directional drilling (HDD) application has evolved worldwide, by giving consequent solutions to major operational, safety, and economic challenges. Previous studies have predominantly focused on hidden failure models and post failure investigations with limited emphasis on a comprehensive understanding of multifactor interactions governing drill pipe failure under actual field conditions. A systematic analysis of drill pipe failure addresses this gap by presenting an integrated assessment of material characteristics, mechanical performance, and operational factors. This gap emphasizes the need for a critical review of the available research to support developments in drill pipe design, material engineering, operational parameters, and predictive failure assessment in HDD applications. Practical insights for failure mitigation and to contribute to safer and more cost-effective HDD operations are expected to be achieved through the outcomes of this study.

TABLE 1 Drill pipe performance characteristics.

Characteristics	S-135	G-105
Outer diameter (m)	0.127	0.127
Inner diameter (m)	0.108	0.108
Pipe size and weight (Kg/m)	0.127 × 8.845	0.127 × 8.845
Torsional strength (N-m)	100,466.109	78,139.856
Tensile strength (kN)	3167.45	2463.57
Collapse capacity (MPa)	108.054	89.624
Burst pressure capacity (MPa)	117.934	91.727

TABLE 2 Tool joint performance characteristics.

Characteristics	S-135	G-105
Outer diameter (m)	0.168	0.168
Inner diameter (m)	0.069	0.082
Pin tong length (m)	0.228	0.228
Torsional strength (N-m)	85966.992	69752.765
Tensile strength (kN)	6902.33	5644.63
Tool joint/Drill pipe Torsional ratio	0.86	0.89

This review paper gives solid observations of drill pipe failures in HDD operations, with significance on identifying dominant failure mechanisms, surveying the influence of drilling loads and environmental conditions, and summarizing material and structural factors that govern drill pipe performance. It organizes and critiques key research findings, highlights major knowledge gaps, and outlines future research scope needed to enlarge the reliability, safety, and longevity of drill pipes used in HDD. A summary of compelling studies on HDD drill pipe failures is presented to provide an understanding of current challenges and support the progress of more prosperous analytical and design approaches. In recent years, existing literature shows us that machine learning models have also developed to predict the drill pipe failure using Real time Data analytics and AI (Machado et al., 2022).

TABLE 3 Summary of studies on failure of drill pipes during Horizontal directional drilling.

References (year)	Title of manuscript	Type of failure	Approach	Remarks
Li et al. (2011)	Failure analysis of 127 mm G105 drill pipe	Decarburization	Micro fractography, optical metallography, optical microscopy	<ul style="list-style-type: none"> A 0.35 mm thick white layer, mostly composed of ferrite and exhibiting surface fissures from decarburization, was observed, along with significant reductions in surface hardness and fatigue strength Drill pipe's heat treatment technique must be altered
Willersrud et al. (2015)	Fault diagnosis of down hole drilling incidents using adaptive observers and statistical change detection	Washout	Generalized likelihood ratio test (GLRT)	<ul style="list-style-type: none"> Uses the noise distribution in the calculated parameters to best suit a t-distribution Early detection will aid in the resolution of the problem
Ma (2004)	Fatigue of drill pipes used in horizontal directional drilling	Fatigue	Stress-life (S-N) approach, strain-life approach and the linear elastic fracture mechanics (LEFM) approach	<ul style="list-style-type: none"> Pipe joint is the weakest point in the pipe Surface hardening can be employed to increase the fatigue life
Cao (2011)	Research on fatigue mechanism and fatigue life of the drill pipes used in horizontal directional drilling	Grain boundaries	Microstructure Refinement	<ul style="list-style-type: none"> Usage of Hall-Petch relationship Grain refining leads to an increase in the yield strength of steel; postpone the emergence of fatigue cracks
Zhu (2016)	Failure analysis and solution studies on drill pipe thread gluing at the exit side of horizontal directional drilling	Bending moment	Finite elemental analysis	<ul style="list-style-type: none"> Bending moment cannot be applied to 2D models An angled shoulder thread capable of withstanding a greater bending moment is presented
Fangpo et al. (2011)	The development and experimental study on high strength and toughness drill pipe steel	Fracture and piercement	Deforming hot rolling process	<ul style="list-style-type: none"> To obtain ultrafine grain microstructure, a large deformation hot rolling method was applied Fine carbides are dispersed to improve steel fracture toughness
Li et al. (2013)	Galling failure analysis of drill pipe rotary shouldered thread connections for horizontal directional drilling	Galling	Optical metallography, spectroscopic chemical analysis	<ul style="list-style-type: none"> Galling can be avoided by coating threads with ion-plated films Quality inspection of pipes
Li and Xin (2011)	Simulation technology in failure analysis of drill pipe	Axial forces	Mechanical simulation	<ul style="list-style-type: none"> The transitional zone's round corner is where stress concentration is at its highest level Tool joint usage
Vlasiy et al. (2017)	Improving the stability of aluminum drill pipes by optimizing the shape of the protector thickening	Torque	Mathematical modeling	<ul style="list-style-type: none"> The stability of the drill string can be strengthened by using aluminum drill pipes with a protective thickening of streamlined contour Calculation of ideal make-up torque
Chunjie and Tie (2009)	The research on axial vibration of drill string with delphi	Axial Vibration	Delphi software	<ul style="list-style-type: none"> Natural frequency of axial vibration is found
Fedorova et al. (2020)	Improving the drill pipe durability by wear-resistant surfacing	Wear and corrosion	UCFT, MAO	<ul style="list-style-type: none"> Hard banding is applied by electric welding to the drill pipe

2 Drill pipe failures during the horizontal directional drilling

2.1 Drill pipe failures due to decarburization

Decarburization is the decline in the carbon content in the material's surface-adjacent zone, and it occurs when carbon atoms on the drill pipe's steel surface contact the drilling environment and are released in the gaseous phase from the steel. From high to low concentrations, carbon diffuses to the surface from the interior until the maximum decarburization depth is reached. Since the structure is fully austenitic,

the maximum affected depth (MAD) grows as temperature rises above a specific threshold because the carbon diffusion rate rises with temperature. Temperature and composition determine different carbon diffusion rates between ferrite and austenite (Voort, 2015).

Decarburization is a significant issue since the surface qualities are sub-par compared to essential qualities, as low wear resistance and fatigue life. Two significant characteristics that may be found on the surface of decarburized steel include the free-ferrite layer (FFD, when free-ferrite is present) and the partial decarburization depth (PDD, when free-ferrite is missing). Light microscopes are used to look for what seems to be the largest depth of entire carbon loss

(free-ferrite depth, or FFD), as well as the highest depth of combined FFD and partial carbon loss, on the surface of a polished and etched cross-section to determine MAD (Voort, 2015).

The wear and fatigue life of drill pipe steel heat-treated components is decreased by decarburization (Voort, 2015). The surface material's organizational state may be altered by the decarburization phenomena that result from drill pipe upset, which can greatly reduce the material's strength and fatigue properties and increase the production of fatigue cracks (Fangpo et al., 2011). The period of fatigue fracture initiation diminishes as the depth of the decarburized layer increases. When the depth of the decarburized layer reaches a specific depth, the initiation life of a fatigue fracture is considerably reduced. The surface decarburized coating accelerates fatigue crack initiation and lowers drill pipe service life. The drill pipe surface hardness was decreased by the decarburization layer, which also helped to produce the surface damage (Guang-sheng and Hong, 2007).

Drill pipe premature fatigue fracture occurs during the drilling operation as a result of the surface decarburization layer's significant reduction in the fatigue crack initiating life (Fangpo et al., 2011). The decarburization surface can result in the formation of numerous microscopic cracks in the drill pipe (Fangpo et al., 2011). Decarburization on the drill pipe's out-surface drastically increased stress concentration, decreased fatigue strength, and led to the development of early fatigue cracks under the action of alternating strain exerted on the drill pipe. The heat treatment method for drill pipes must be modified to inhibit the creation of a layer of surface decarburization (Fangpo et al., 2011). To avoid the creation of a decarburization layer, the upset process of the drill pipe should be improved (Li et al., 2011).

The microstructure, tensile characteristics, and fatigue life of the S135 drill pipe were investigated in relation to the surface decarburization. The results reveal that a surface-decarburized layer significantly reduces material hardness, while having little influence on tensile performance. The period of fatigue fracture initiation diminishes as the depth of the decarburized layer increases. When the depth of the decarburized layer reaches a specific depth, the initiation life of a fatigue fracture is considerably reduced. Surface decarburization causes the creation of corrosion pits on drill pipe surfaces, accelerates fatigue fracture initiation, and lowers the drill pipe service life. To mitigate the negative effects of surface decarburization, the depth of the decarburized layer should be precisely regulated (Li and Wang, 2015).

2.2 Drill pipe failure due to drill pipe washout

A drill pipe washout is a leak from the drill pipe to the annulus brought on by tensile stress or corrosion (Bert et al., 2009). This failure reduces the flow to the drill bit and the lower part of the drilling system, as shown in Figure 2. Figure 2 depicts the drill pipe failure due to washout.

A fault like this might cause the pipe to completely twist off, requiring three to twelve additional days of drilling or, in the worst-case scenario, forcing the well to be abandoned (Macdonald and Bjune 2007). According to earlier research, crevice corrosion, bimetallic corrosion, and differential oxygen concentration corrosion are the main causes of the drill-pipe washout (Fangpo et al., 2011; Liu et al., 2011; Lu et al., 2005). They investigated the

material quality and loading situation of drill pipes in more detail (Lian et al., 2014b; Lian et al., 2014a). Due to the small pressure changes brought on by friction, with no net change in the flow into and out of the well, drill string washout is a complex problem.

Inconspicuous changes in the drilling fluid's pressure and flow rate, brought on by a small washout, are difficult to spot in noisy monitoring data. A washout lessens flow in the drill bit, annulus, and lower parts of the drill string (Willersrud et al., 2015).

FEA analysis implemented was performed on an S135 drill pipe model, which has a yield strength of 1,138 MPa and Ultimate tensile strength of 1,000 MPa. To study the washout observed in the drill pipe, structural constraints are imposed at the ends of the drill pipe.

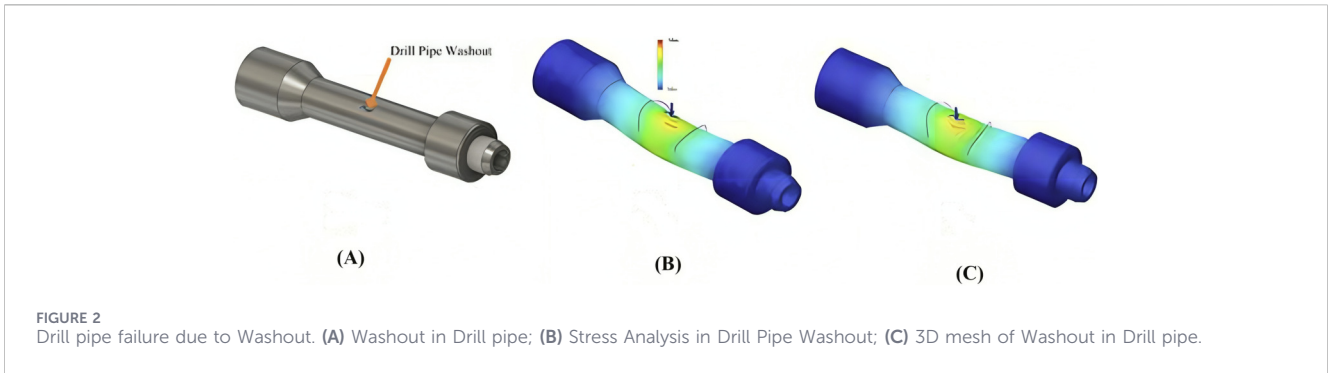
The boundary conditions obtained using FEA analysis are as follows:

- Von Mises stress: 0.002657 MPa (Minimum) and 3,707 MPa (Maximum);
- Total displacement: 0.6988×10^{-3} m.

These values represent localized peak responses and should not be interpreted as typical material strength limits under normal HDD operations.

2.3 Drill pipe failures due to fatigue

Fatigue is a cumulative and irreversible phenomenon caused by repeated cyclic bending loads and stresses in tensile or buckling drill pipes (Sikal et al., 2008). A structure fails due to fatigue when it is subjected to constant loads. Studies show that fatigue in drill pipes, which manifests as joint-thread fracture, pipe fracture, welding-line fracture, and other symptoms, accounts for more than 80% of drill pipe failure in HDD. Fatigue failure occurs when stress is at its highest and intention is at its lowest. For drill pipes, the first place where a fatigue fracture occurs is where there is a concentration of stress, such as machining cutting marks, carrying scars, and slip clipping marks (Cao, 2011). A fatigue fracture will have two distinct regions: one smooth as a consequence of the rubbing of the bottom and top of the crack, and one granular caused by the material's quick failure. Scratches and other surface defects will reduce the fatigue life of a material. Chemical attack or corrosion causes the creation of microscopic pits on the material's surface. The immersion of drill pipes in flowing drilling mud tends to shorten their fatigue life. The steel grade used in the pipe has a considerable effect on the drill pipe's fatigue life; in this regard, steel fatigue life can be attributed to its tensile strength. Fatigue in HDD is mostly induced by bending stress caused by drill rod curvature and rotation. The strain is the greatest in a small area of the cross-section. The higher the steel hardness, the greater the fatigue performance. Fatigue failure can be classified into two major categories based on the rate of propagation to failure due to fatigue. High-cycle fatigue and low-cycle fatigue are the two forms of fatigue. There is no sharp distinction between the two regimes. The high-cycle fatigue is distinguished by a high number of cycles to failure, with life represented by S-N curve data. If there are no faults at the beginning, the majority of the performance life is spent in the crack initiation phase, whereas the low-cycle fatigue is defined by failure in a short number of cycles i.e., considerable plastic deformation with each cycle, strain versus the number of cycles explains fatigue behavior and separate power-law



correlations are employed for the elastic and plastic components of the strain. Drill pipe rupture is likely to occur immediately after a fatigue crack is discovered in the field (Ma, 2004). It is possible for impurities and the second-phase particles, produced during the smelting of pipe materials, to break apart or fracture, leading to the development of a crack between the body material and the impurity. In smooth drill pipes, slippage results in a fatigue crack. Despite having the slip lines that are unevenly distributed and only occur in a small area, some pipe material grains are oriented in the maximum shear plane, which is easily slipped. As the initial slip line slippage increases with fatigue, a new alongside slip line appears, resulting in the slip bands. As the slip bands deepen and spread, “Invading Ditch” and “Extruding Ridge” appear on the pipe’s surfaces. These are the crack origins; the break spreads in the sliding direction, passes through the grain, and creates a macro crack (Cao, 2011). The crystalline interface develops a slip band when materials are kept at high temperatures. Surface asymmetry is a macro and micro surface fault that develops on drill pipe bodies due to poor management, improper operating usage, and, especially notable, slide cuttings. In the drilling industry, these areas are commonly recognized as fatigue fracture starting points (Macdonald and Bjune 2007; Rahman, 1999; Rahman et al., 1999; Simpson et al., 2004). Some cracks that began close to the slip-crushing locations resulted in a wash-out samples having slip-cuts at thick as 0.1–0.4 mm all over its exterior. Rotation of the drill pipe during the slide landing could result in extremely hazardous marks around the periphery of the drill pipe. Drillers and tool pushers should refrain from carrying out this kind of operation. As fatigue worsens, slip bands at grain boundaries cause greater strains, which causes dislocation to accumulate in front of grain boundaries. Grain boundaries break whenever the stress from displacement stack is greater than the anticipated fracture strength. The dislocation pile-up is larger and fracture formation is easier when there is more pressure on the grain boundary. According to the above-mentioned research, the difficult working conditions endured on the drill pipe near the reamer caused significant alternating stress, resulting in the commencement of fatigue fractures on the drill pipe’s surface. As the fissures spread, the remaining wall thickness became too weak to withstand the reaming torque, and the drill pipe fractured.

2.4 Drill pipe failures due to grain boundaries

A grain boundary is a planar defect that develops when two such crystallites meet. Both sides have an identical crystal structure and

chemical content, but the orientation differs. Grain boundaries are critical to understanding deformation and fracture mechanisms in a variety of materials (National Research Technological University “MISIS” et al., 2020). If the two are considered to have a single origin, the transformation between them is a pure rotation, which is known as Misorientation. Misorientation impacts the boundary’s properties, such as surface tension, mobility, and stiffness, and is thus critical in the research of grain boundaries, particularly in the case of drill pipe material. Coarse-grained metals typically bend plastically due to dislocations and line defects of the normal crystal lattice inside individual grains. Dislocations within crystal grains can pass through them and communicate with one another (Velikov et al., 2002). Grain boundaries typically prevent their transmission, which leads to a dislocation pile-up at the border and makes the material more difficult to deform (Van Swygenhoven, 2002). This is possible in the case of a steel drill pipe. The slip band at the crystalline interface is restricted when materials are maintained at high temperatures. Slip bands near the grain boundaries lead to increased strains as fatigue progresses, which leads to an accumulation of dislocations in front of grain boundaries. When the tension from a dislocated stack exceeds the expected fracture toughness, intergranular rupture. The grain boundary is more distressed (Li et al., 2022). It is easier for cracks to form at the boundary when there is a bigger dislocation pile-up (Cao, 2011). Aluminium alloy drill pipes were chosen as the material system for the drill string in ultra-deep well drilling engineering because of their low density, high specific strength, and deep drilling depth. These had frequently been incorporated into the planning of horizontal wells, incredibly deep wells, and difficult drilling sites (Gwilliam, 1999; Lv et al., 2009; Yan et al., 2010). Aluminum alloy drill pipes can have some disadvantages, though, such as their low hardness, quick attrition, and low resistance to salt corrosion, which can cause failure from corrosion and wear (Liang et al., 2018; Sun et al., 2011; Tang et al., 2011; Varma and Vasquez, 2003).

2.5 Drill pipe failures due to bending moment

The bending moment is defined as the change in shape and form generated by internal and external stresses and pressures in a drilling pipe, as shown in Figure 3 (Hawkins, 2005). Figure 3 depicts the drill pipe failure due to the bending movement. The principal load carried by the drill pipe is the bending moment (Zhu, 2016). The drill pipe’s bending deformation is caused by the bending moment

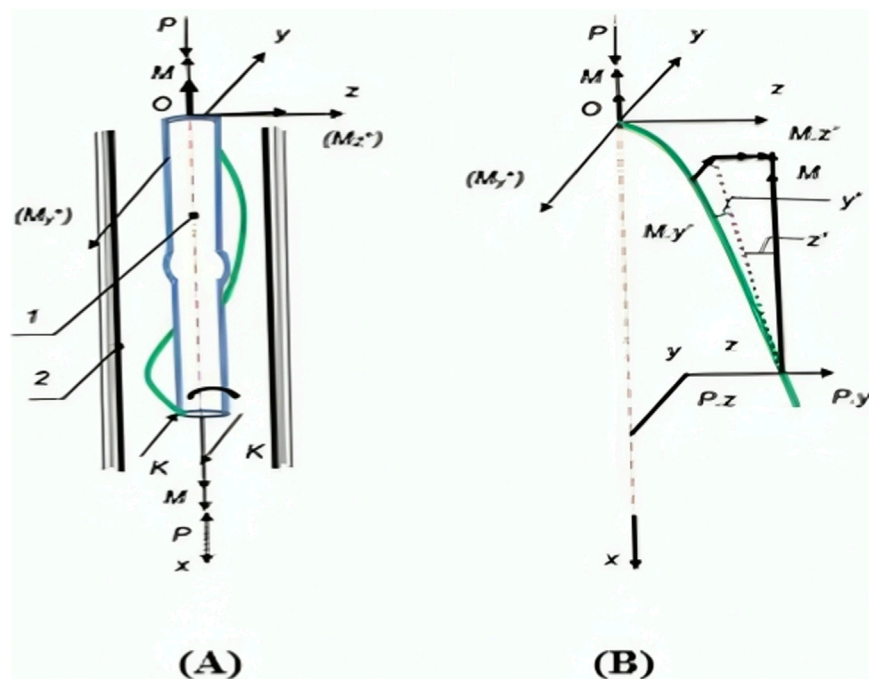


FIGURE 3
Drill pipe failure due to Bending Moment. (A) Bending Moment in Drill pipe; (B) 3D mesh of Bending Moment in Drill pipe.

(Cao, 2011). The drill pipes experience bending moments while drilling, both in the bending zone and the curving hole. As the drill pipes rotate, the alternate bending stress is introduced. In its bent state, the drill pipe rotates around its axis, creating alternating bending stress (Cao et al., 2009).

The implemented FEA analysis was performed on a S135 drill pipe model with a yield strength of 1,138 MPa and a tensile strength of 1,000 MPa. To study the bending moment, structural constraints are imposed at the ends of the drill pipe. The boundary conditions obtained using FEA analysis are as follows:

- Von mises stress: 59.73 MPa (Minimum) and 26,718 MPa (Maximum);
- Total displacement: 126.3×10^{-3} m.

The drill pipes could bend due to the following factors:

- The provided pressure is greater than the drill pipe's critical bending stress;
- Weight-induced drill pipe distortion due to bending;
- While drilling, the centrifugal force drives the drill pipe to bend.

The drill pipe is bending as it operates, borehole during the directional drilling operation, causing bending deformation (Cao, 2011). When the bending moment occurs, the portion of the thread attachment is now in tension, and the other is in pressure. On the shoulder, greater contact stress and Mises stress zones are often located on the tension face and are distributed unevenly around the circle. The engaged thread may become stuck and develop shoulder galling as a result of the increased bending moment (Zhu, 2016).

2.6 Drill pipe failures due to fractures and piercing

Fracture and piercing of drill pipes are the two most frequent types of failure. A fracture frequently results in drill equipment falling into wells, which generates higher financial losses than piercing. The piercing can be identified, though, by a shift in the drilling fluid entrance pressure, and the leaky pipes can then be swiftly changed. Because of this, the researchers predict that the piercing will occur before the fracture. The most crucial factor in determining the type of failure of drill pipes, in accordance with the fracture mechanics theory, is toughness. The size of the fatigue area surpasses the thickness of the drill pipes when the toughness rises above a critical value, leading to piercing. When the toughness is below the significance threshold, however, the fracture occurs immediately. Thus, increasing toughness while maintaining adequate strength is one of the best ways to assure the security of drilling operations. In due course, drill pipe steel of high strength and hardness is being prioritized by makers of drilling tools (Lu et al., 2005; Baryshnikov et al., 1997; Dale, 1988; Hansford and Lubinski, 1966). The high-strength steel, used to make drill pipes, commonly runs into this problem: if the drill pipes are made using the hardening and tempering process, a higher strength frequently results in a lower toughness, and the yield ratio tends to fall. Therefore, a novel technology to enhance strength, toughness, and yield ratio must be created (Xu et al., 2011).

2.7 Drill pipe failures due to galling

Galling is a type of adhesive wear that happens most commonly in the presence of relatively high stresses. Galling failure has

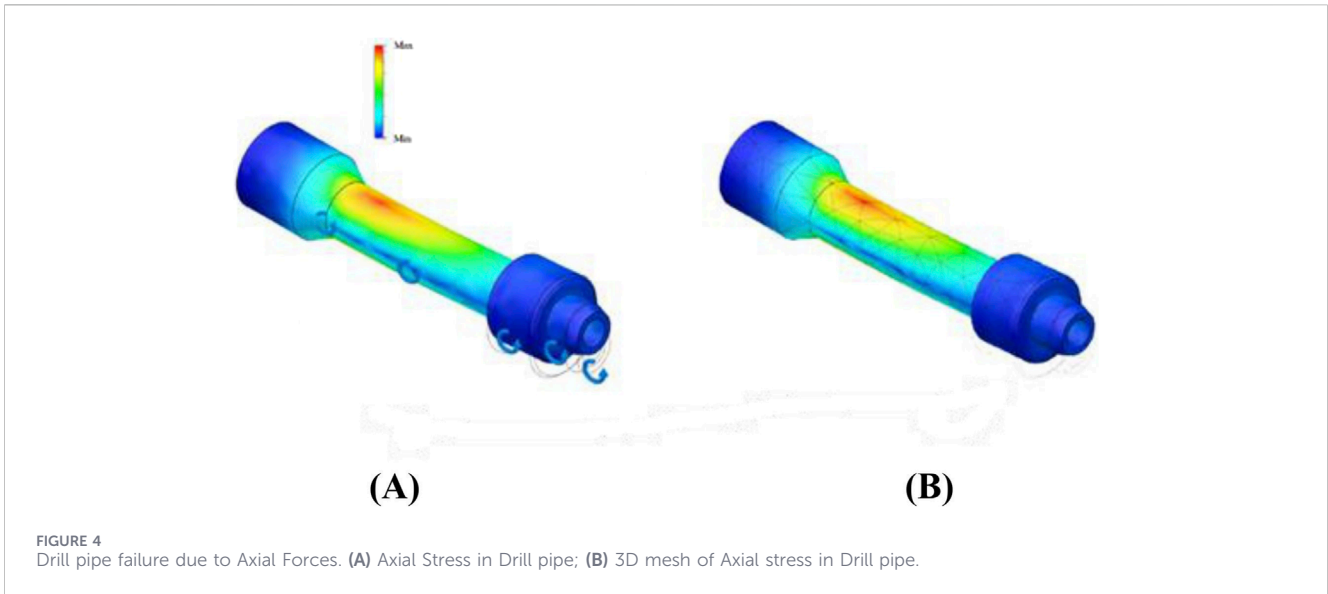


FIGURE 4
Drill pipe failure due to Axial Forces. (A) Axial Stress in Drill pipe; (B) 3D mesh of Axial stress in Drill pipe.

traditionally occurred on threaded components. Galling is highly related to lubricity since galling happens following lubricity breakdown. To prevent galling, lubricants are widely utilized. As a consequence, it is worth considering the role of boundary-layer films in lubricating (White, 1984). Failure incidents hurt the standard of Horizontal directional drilling in addition to causing drill pipe to be abandoned. The galling breakdown phase of rotary chested thread connections is significantly influenced by thread specifications, compound efficiency, drill string helical bucking, and make-up torque. To avoid galling failure accidents, controlling compound quality and adequate field operation are necessary. A few tool joints and a few thread compounds can be examined to discover the source of the rotary-shouldered thread connection's galling failure (Li et al., 2013).

2.8 Drill pipe failures due to axial forces

An axial force is a force that applies perpendicularly to the cross-section of the drill pipe (Figure 4). Axial forces are categorized as tensional or compressive. This force's compression causes axial stress. The pulling force (pressure) of the rig and the friction force of the hole wall combine to create the axial force of the drill pipes (Cao et al., 2009).

FEA analysis was carried out on a S135 drill pipe model with a yield strength of 1,138 MPa and an ultimate tensile strength of 1,000 MPa. To study the axial stress, structural constraints are implemented at both ends of the drill pipe. The boundary conditions obtained using FEA analysis are as follows:

- Von Mises stress: 2.364 MPa (Minimum) and 1,270 MPa (Maximum);
- Total displacement: 0.2826×10^{-3} m.

Many parameters influence axial force transfer: coefficient of friction, operating circumstances, well trajectory, buckling, drill string features such as tool-joint, stiffness, stabilizers, and so on. Tensile axial loading and compressive axial loading are the stresses

induced by axial forces in drill pipes. Tension in the drill pipe arises primarily during the pullback due to frictional forces on the drill string and product pipe, and resistive forces at the reaming assembly's cutting face. During the pilot hole boring procedure, drill pipe compression generates thrust for the drill bit. As previously stated, since the drill pipe is very slender in comparison to its length, it is likely to buckle and will be restrained by the borehole walls. Drill pipe buckling often takes the form of helical buckling. Axial forces in the drill pipe are caused by the compressive push during drilling and tensile pressure during withdrawal, resulting in coupled cyclic loads (Zhu, 2016).

2.9 Drill pipe failures due to torque

A measure of the force that propels an object around an axis is called torque. Torque is the quality that causes an object to obtain an angular acceleration, similar to a force that causes an object to accelerate in terms of kinematics. Torque is a vector value, also known as a moment. The direction of force about the axis has a significant influence on the torque's vector direction (Ma et al., 2005). Drilling for wells uses a rotating technique. The transmission of chisel torque from the surface-based rotor, or a turbodrill, or an electric drill, inserted in the drill pipe column, provides an axial load (Cao, 2011). The drill pipes are subjected to torque during drilling. The top of the hole has the most torque, whereas the bottom has the least torque (Cao et al., 2009). Over-torquing often occurs when the drill pipe under under-torqued prior to its run down the hole. The pipe down the hole might easily be overtightened under these circumstances. When the pipe is pushed underground onto a curved path by providing the required torques to rotate the drill bit, flexural stress and torsional stress are produced (Ma et al., 2005). Under the standard torque, also known as makeup torque, needed to complete a connection in the drill string, the contact stresses of the initial engaging turn and shoulder diffused evenly around the concentric plane. The minimal contact stress between the shoulder and the first engaged turn when the make-up torque is 6,000 Nm is 33 MPa. Leakage during operations could result in

thread gluing mishaps throughout the construction process because sealing failures allow high-pressure drilling fluid to enter the engaged screw and increase friction (Cao et al., 2009). Due to its weight, the drill pipe string will rotate both along its own axis and the axis of the borehole if the horizontal distance of the directional drill is too vast and the diameter of the hole is much larger than the drill pipe's outer diameter. The drill pipe's outside is consequently subject to alternating stress. During the reaming operation, the drill pipe that connects to the reamer spins around the fixed-point reamer, putting the drill pipes closest to the reamer under the highest strain and accelerating the formation of a fatigue crack. As the crack spread along the wall thickness to a certain amount, the carrying capacity of the drill pipe would be diminished. Finally, the drill pipe's reamer develops an over-torque fracture (Lu et al., 2011).

2.10 Drill pipe failures due to torsional vibration

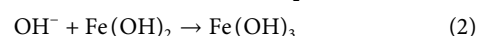
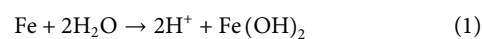
The oscillatory twisting of shafts in a rotor assembly that occurs in tandem with the running speed is known as torsional vibration. The frequency could be an eigenvalue, or it could be pushed externally. Resonance will develop if a forcing frequency and a natural frequency coincide. A turbo machine's individual rotors are frequently robust enough in torsion to operate beyond the typical torsion excitation frequency range. Torsional vibrations might result in erratic downhole rotation. Stick/slip is a severe form of drill string Torsional oscillation in which the bit becomes motionless for a period of time. The length of the stuck period increases as the severity of the stick/slip increases, as do the rotational accelerations as the bit comes free. Geological heterogeneity can modify the drill bit's rotational resistance, resulting in torsional vibration and alternating transverse stress in the drill pipe. Drill bit structure, geological conditions, drilling pressure, rotating speed, and other factors all have an impact on the alternating transverse stress (Cao et al., 2009). Torsional variations have the potential to break bits and harm drill collar connections. If the bit is the predominant source of excitation, the use of a mud motor may help minimize stick/slip, but a motor by itself does not do so. Even though the bit is running at a steady pace; thanks to the motor, the drill string and BHA above the motor may start to stick or slip. In addition, since drill string is an under-actuated system with a very tiny diameter to length ratio that is driven at one end and cut at the other, torsion oscillations in the drill string are particularly challenging to control. These qualities make the drill string more prone to self-excite. Torsional vibrations brought on by the stick-slip of the cutting bit, designed as a system with two degrees of freedom, a torsional pendulum with the top drive, and some drilling pipes represented by the upper inertia (Ullah et al., 2016). The bottom hole assembly is represented by bottom inertia (BHA). An analogy for the drill is a massless torsional spring damper. A dry friction model is used to simulate the friction that the drill string encounters. The Stribeck effect, stiction, and Coulomb friction are all taken into consideration by the friction model. The main nonlinear event at the bit that causes negative damping and self-reinforcing stick-slip Torsional oscillations is the latter friction component.

2.11 Drill pipe failures due to axial vibration

Drilling engineering is significantly impacted by the frequent occurrence of drill string vibration. Drill string resonance is the primary factor in drill string fatigue. Axial, lateral, and torsional vibration are the three basic types of drill string vibration in the drilling engineering process. The natural frequency is crucial for drilling personnel because the resonance of the drill string's axial vibration is extremely harmful to drilling. Many drilling accidents are caused by high axial vibration, such as bounced bits and damaged drill strings. Axial vibration occurs more easily than other types of vibration; axial vibration of a roller bit has a significant impact on drilling engineering, whereas axial vibration of a drill string has a negative impact on the bit and tie-in (Chunje and Tie, 2009).

2.12 Drill pipe failures due to wear and corrosion

Corrosion fatigue cracks in drill pipes are caused by the tension of alternating stress and corrosive media. The drill pipe failure is influenced by stress situation, corrosion, and stress accumulation in the drill pipe construction. According to the test results of Lu et al. (2005), Corrosion pits are the source of corrosion fatigue fractures, and pits and cracks are substantial in taper inner upset zones, vulnerable to a sudden change in geometry. The corrosion pits show pinhole corrosion. This implies that tiny batteries with Fe anodes initially form in discontinuous regions of the metal microstructure, such as inclusions, outcrops of streamline metal, carbides, and structural discontinuities, including roughness and sudden structural changes, at the internal upset taper location. Corrosion begins to occur as Fe dissolves. The hydrolysis of Fe ions is as followed by the Equations 1, 2:



Since Fe(OH)₃ formation occurs at corrosion pits and encloses pitheads, the pH drops as Fe and H⁺ ions dissolve rapidly. At the same time, Cl⁻ in mud enters pits through pitheads due to ionization and reacts to form hydrochloric acid as followed by Equation 3:



This causes pH to decline, and the solution moves faster. In other words, there is catalytic action. Although the absence of visible streamline metal for the equivalent drill pipe, the longitudinal section contained severe streamline metal, with the streamlined metal at the inner surface being more severe than that near the surface of the environment. Therefore, failed drill pipes must show the discontinuous configuration in micrography as well as discontinuous microstructure (like bandings, inclusions, carbonizations, and so forth). The drill pipe's inside surface was covered in numerous corrosion pits. The area with the largest pits also had the largest fatigue cracks. Due to the mud's presence of dissolved oxygen, chlorine, and other components, corrosion concentrations formed at points along the internal upset taper that were vulnerable to sudden changes in geometry. Drill pipe erosion can be effectively avoided using internal surface coating.

Since drill pipes were submerged in mud with Cl^- and dissolved oxygen, while being drilled, extensive corrosion must have occurred on the inside surface of the drill pipe at points vulnerable to sudden variation in geometry. Corrosion of drill pipes can be effectively avoided by applying an internal surface coating. As corrosion pits develop and corrosion fatigue fractures start and spread, the concentration of stress rises. According to the test results, the cracks are only present in internal upset taper regions that are vulnerable to abrupt geometric alterations. The internal upset taper section is at a weak point, and the sudden geometric changes in the structure hasten the beginning and progression of corrosion fatigue cracks (Lu et al., 2005). The drill pipes failed prematurely as a result of corrosion fatigue cracks. The well's rigorous condition, which includes a severe corrosion medium, a dog-leg, an evident tilted angle, as well as the drill pipe's poor quality with an erratic internal upset taper arrangement vulnerable to rapid geometric change, was the main cause of drill pipes washing out (Lu et al., 2005).

The results of Li and Wang (2015) reveals that the surface decarburized layer significantly reduces material hardness. The period of fatigue fracture initiation diminishes as the depth of the decarburized layer increases. When the depth of the decarburized layer reaches a specific depth, the initiation life of a fatigue fracture is considerably reduced. This surface decarburized layer encourages the creation of corrosion pits on the drill pipe's surface, accelerates the beginning of fatigue cracks, and decreases the drill pipe's service life.

3 Analysis of drill pipe failure during horizontal directional drilling

3.1 Analysis of drill pipe failure due to decarburization

Fangpo et al. (2011) investigated inspection of the drill pipe's configuration, chemical makeup, mechanical performance, metallography, and microfractography. Researchers had analyzed the mechanism of crack propagation under fatigue stresses in relation to external and internal parameters using micro fractography, which is the inspection of a fracture surface under high and ultra-high magnification using an optical or electron microscope. Micro fractography seems to be very well suited for studying cumulative damage and determining the cause of service failures (Jacoby, 1966). Metallography is the study of the microstructure of all types of metallic alloys. Spectroscopic chemical analysis was used to determine the chemical makeup of the drill pipe body. Drill pipe is made of 25CrMnMo steel, phosphorus, and sulfur. Mechanical properties were evaluated using impact testing equipment and an MTS machine. Optical metallography was used to investigate microstructures. The crack surface was examined using both SEM and visual inspection. Visual inspection confirmed that the piercing point was far from the start of the internal upset tape and that the protective coating on its interior surface was not damaged. Mechanical damage was spread uniformly throughout the cracks. Optical microscopy investigations revealed that numerous mini-cracks, known as fatigue cracks, developed and spread straight. A white layer, primarily composed of ferrite, with surface cracks caused by decarburization. The Vickers method was

used to compute the depth of the decarburization layer. Microhardness tests revealed a 0.35 mm decarburization layer that caused numerous fractures. Fracture (Fatigue) striation bands were seen at high magnification, and there is clear corrosion evidence on the fracture origin and root level morphology of fatigue fracture. The fracture surface was coated with O, Fe, Si, and trace amounts of C, Ca, Na, and Cr, according to the results of the spectrum investigation (Fangpo et al., 2011). When there is decarburization, the hardness of the surface and the strength of fatigue are significantly reduced. The bottom-most surface damage microcrack started to extend trans granularly in a straight line. The outer layer of the drill pipe experiences surface decarburization, which modifies the organizational state of the surface matter, lessens its toughness and strength and encourages the development of corrosion and scratches. After seamless tubular hot rolling, a quenching and high-temperature tempering method was performed to ameliorate the mechanical properties of the drill pipe body and reduce high residual tensile stress. A protective coating was sprayed on the inside surface to prevent it from failing due to corrosion. Drill pipe fatigue life depends on fatigue fracture initiation time and the fatigue crack propagation time, with the former accounting for the majority of the latter. The premature fatigue crack of the drill pipe was induced by surface decarburization and mechanical degradation. Due to improper heat treatment, a decarburization layer formed on the outer layer of the drill pipe, which led to failure. Attributable to the alternating stress during the drilling operation, this layer significantly decreased the drill pipe's fatigue resistance and accelerated the formation of fatigue fractures, ultimately causing drilling pipe washout failure. A surface decarburization layer must not form during the heat treatment process of the drill pipe to avoid such failures. Efficacious precautions should also be provided to avert mechanical damage (Fangpo et al., 2011).

3.2 Analysis of drill pipe failures due to drill pipe washout

Drill pipe washout is one type of fatigue failure accident that must be avoided. For assessing the failure, inspect the design of the drill pipe, chemical composition, metallography, and Micro fractography (Fangpo et al., 2011). It was discovered in the paper that the washout failure of the drill pipe body is a premature fatigue failure. Failure was caused by a layer of decarburization on the outer zone of the drill pipe as a result of inadequate heat treatment, which significantly reduced the fatigue resistance of the drill pipe body. Variable loads prompted fatigue cracks in the decarburization layer to develop swiftly. The drill pipe washed away as fractures spread along the thickness of the wall (Fangpo et al., 2011). The degree to which friction characteristics changed is affected by the amount of the washout, although the immensity of change is unknown. It is critical to diagnose a drill stem washout as soon as possible (Willersrud et al., 2015). As a consequence, changes can be detected by a generalized likelihood ratio test (GLRT). To best fit a t-test, GLRT employs the frequency distribution in the derived specifications (Willersrud et al., 2015). To pinpoint downhole drilling errors, the research suggests employing statistical change detection tools. It is very beneficial to locate the exact site of the defect to improve the effectiveness of inspection and replacement, in



FIGURE 5

Technique for failure analysis with an adaptive observer and statistical variation detection, where $\hat{\theta}$ denotes projected attributes, y denotes measurements, and $\Delta\mu(\hat{\theta})$ denotes a change in the mean of the projected attributes.

addition to pinpointing where the washout occurred (Willersrud et al., 2015). The recommended approach, shown in Figure 5, entails estimating a set of friction characteristics using a nonlinear adaptive observer and a mathematical model that is comparatively simple, followed by integrating the above mentioned using specialized change recognition. Computed specifications stay (or almost remain) the same throughout routine operation; however, they will vary if a washout occurs in a system. The diagnostic method is validated using inputs from a moderate-sized flow cycle constructed and certified by Equinor ASA (formerly known as Statoil ASA). The friction estimations are demonstrated to be considerably impacted by noise in the data. Investigating alternatives for identification and exclusion is due to changes in estimated variables that take place during the washout. Based on the GLRT methodology, dedicated change detection techniques for the observed multivariate t -distribution are developed. Nonetheless, the current method has proven adequate to enable compelling detection of washout and separation of the leaking point (Willersrud et al., 2015). Due to the early onset of the washout problem, early detection will aid in the resolution of the problem.

3.3 Analysis of drill pipe failures due to fatigue

Surface hardening is a surface treatment used to increase the hardness and fatigue life of a material. This is accomplished by subjecting the component to a high-temperature carbon-rich environment. Carbon diffuses into the material, filling interstices and other voids up to 1 mm in depth. Equations 4, 5 is used to find fatigue life in terms of cycles (N),

$$\text{Log}N = 14.8 - 3.46 \log S_r - 16.5 \cdot 10^{-5} (S_m)^2 \quad (4)$$

where S_r refers to stress range in MPa, and S_m refers to mean stress in MPa.

If the mean stress is zero for the case of bending,

$$\text{Log}N = 22.28 - 3.46 \log S_r \quad (5)$$

It is challenging to provide a straightforward analysis of the expected fatigue life because the rod will be bent into a different curvature and subjected to varying axial and torsional stresses for each use. The Palmgren-Miner linear damage summation rule can be used to address various cyclical stress conditions, which is given in Equation 6:

$$d = \frac{2n_i}{2N_{f_i}} = \frac{\text{Reversals at } \sigma_{ai}}{\text{Reversals to failure at } \sigma_{ai}} \quad (6)$$

where $2N_{f_i}$ refers to the number of failed reversals at σ_{ai} , d refers to partial damage for each loading σ_{ai} . The summation rule assumes that the order in which the loads are applied does not affect the component's lifetime. In reality, the sequence of loads can have a significant impact on the component's lifetime. The three main fatigue failure models include the stress-life (S-N) approach, the strain-life approach, and the linear elastic fracture mechanics (LEFM) approach. The stress-life method is a stress-based model that aims to identify the material's fatigue strength and endurance limit to reduce cyclic stresses below that level and prevent fatigue failure for the necessary number of cycles. This approach is frequently applied to high-loop fatigue, where the number of stress loops is predicted to be more than 1,000. Local stresses in any notch are kept so low in this manner. Since the loads and strains remain in the elastic zone everywhere, local yielding precedes creation of a crack. The strain-life methodology is a strain-based model that provides an accurate estimate of the crack-initiation stage. This method is frequently used for the low-cycle fatigue and finite life problems involving cyclic stresses high enough to cause yielding. The best model of the crack propagation stage of the process is provided by fracture mechanics theory. This method is used to predict the remaining life of cracked components in Low cycle fatigue (LCF) and finite life situations.

The majority of fatigue failures are observed to occur in the joint area, which might be due to poor processing, but it could also be due to less-than-ideal curvature and stress conditions during boring and reaming operations. This shows that the pipe joint is the weakest point in the pipe. Although a redesign of the joint may increase performance, the number of revolutions to access joint failure is based on the radius of curvature. This study helps to provide a well-balanced design based on fatigue resistance (Sun et al., 2024). It is crucial to avoid stress concentration in the transition zone when constructing a friction-welding drill pipe connection. High-cycle fatigue is normal due to increased stress during HDD (Ma et al., 2005).

3.4 Analysis of drill pipe failures due to grain boundaries

Microstructure refinement is a cost-effective and efficient way of resolving grain boundary issues and enhancing strength and toughness to avoid fracture and piercement (Cao et al., 2007; Chen et al., 2009). The addition of alloy components helps us to refine the size of the grain. (Xu et al., 2011). involves the use of Niobium (Nb), a strong former of carbide that is frequently used in high strength low alloy steels for grain size refining and for modification of characteristics. Nb is more soluble in austenite

than in ferrite, and its solubility increases with temperature. In micro-alloyed steels, Nb has been shown to have the largest solute-strengthening impact, and concomitant additions of V and/or Mo have been demonstrated to enhance this effect (Cao et al., 2007; Charleux et al., 2001). Strengthening of high solute enhances the nucleation rate for recrystallization and raises the distortion energy during hot deformation. Nb in solid solution can also significantly slow down the movement of grain boundaries. As the temperature drops, Nb atoms combine to create a large number of nanoparticles that can pin grain boundaries and control the grain size. Appropriate treatment of heat is also required for a well-refined result (Cao et al., 2007; Chen et al., 2009; Lee et al., 2002; Mao et al., 2008). According to Equation 7, the Hall-Petch relationship (Mao et al., 2008) can be used to express the relation between grain size and yield strength.

$$\sigma_s = \sigma_0 + k_y d^{-1/2} \quad (7)$$

where σ_s refers to the elastic limit in MPa, d refers to the mean grain diameter measured in μm , and k_y refers to the Petch gradient, the value of which depends on the structure of the crystal and solute atoms. The elastic limit of steel number 2 rises as a result of grain refinement. The relationship between the size of grain and the critical stress of crack dissemination is described as follows (Mao et al., 2008). Based on fracture mechanics theory on crack formation:

$$\sigma_f = \frac{2Gv_p}{k_y} d^{-1/2} \quad (8)$$

where σ_f refers to the crack propagation critical stress, v_p refers to the interfacial energy (energy used to propagate cracks per square unit), d refers to the mean diameter, G refers to the modulus of rigidity, and k_y refers to the Petch gradient. From Equation 8, it can be found that the ultimate strength improves as the grain size decreases. Furthermore, grain refining can improve the hardness of materials. The small grain slows the onset of cracking by reducing the amount of dislocation accumulation, relieving the concentration of stress at grain boundaries. The relationship between dislocation accumulation and grain size is shown by the empirical equation (Mao et al., 2008), which is stated as:

$$n = \frac{k\pi\tau_s d}{4Gb} \quad (9)$$

where n refers to the amount of dislocation accumulation, τ_s refers to the stress input, and d refers to the diameter of the grain; all other variables are constant. According to Equation 9, the amount of dislocation pile-up decreases as grain size decreases. Furthermore, the fine grain provides greater impediments to crack growth. Consequently, grain refining can improve strength and toughness (Xu et al., 2011). Grain refining can postpone the emergence of fatigue cracks (Cao, 2011).

3.5 Analysis of drill pipe failures due to bending moment

$$M_{\max} = \frac{Ql}{4} \times \frac{tgu}{u} + \frac{\pi^2 EI}{l^2} \times f \quad (10)$$

The estimation of the bending load acting on the drill pipe during HDD is calculated using Equation 10.

The maximum bending stress is calculated in Equation 11:

$$\sigma_{\max} = \frac{M_{\max}}{W_z} = \frac{Ql \times tgu}{4u \times W_z} + \frac{\pi^2 EI \times f}{W_z \times l^2} \quad (11)$$

where W_z refers to the Flexural factor of section, Q refers to drill pipes transverse pressure (Pa), f refers to Space in between the pipes and the hole (m), refers to Instability critical pressure (Pa), EI refers to Flexural stiffness (Nm^2), and g refers to acceleration due to gravity (m/s^2).

According to the study conducted by Zhu, (2016), The drill pipe carries the majority of the bending moment during the HDD process. However, 2D models cannot be utilized to evaluate the bending moment. In order to investigate thread link security under bending moment strain, 2D models are therefore useless. So, a 3D Finite Element Model (FEM) must be used. Fixed limitations are put into the thread's one end, while the bending moment and make-up torque are put onto the other. When the Mises stress distribution of the finite element calculation is compared to the experimental data given by Zhu et al. (2013), both results coincide. Therefore, the results can be considered reliable. If the bending curvature vector length is 14.2 m, the given model predicts that the Mises stresses of the compression side shoulder and first engaged turn are near and substantially over the material elastic limit. The fifth engaged thread turn experiences gluing because the Mises stress of the root of the fifth turn of thread is close to the thread connection's peak stress. This is considerably over the material's fatigue strength on the tension side. This matched the failure situation observed.

The author proposes various improvements based on his examination of drill pipe failure due to bending moment. It proposes hanging of drill pipe support on the exit side. An advanced type of drill pipe thread that can withstand a greater bending moment must be developed. An angled shoulder thread, able to withstand a greater bending moment, is reported (Zhu, 2016). The load is shared on the threaded screw by the structure. This is done by maximizing the contact area of the shoulder, resulting in lower maximum stress upon the screw when the bending moment is operational. Furthermore, under the bending moment strain, the inclined shoulder contacts more closely, which may increase the thread's sealing ability (Zhu et al., 2013). The pitched shoulder thread's highest Mises stress value is nearly 100 MPa less than the API thread's maximum Mises stress value, and the graph between the bending moment and maximum stress value. Figure 6 demonstrates that the Mises distribution of stress of both the structure threads is essentially identical. Pitched shoulder thread may resist more loads of bending moment in the same circumstances because it has a higher bending yield strength than the latter.

3.6 Analysis of drill pipe failures due to fracture and piercement

Hu et al. (2011) created and assessed a novel drill pipe steel in which the C content is reduced and the increased content of alloy elements like Chromium, Nickel, Molybdenum, Niobium, and Vanadium. To obtain an ultrafine grain microstructure, a large

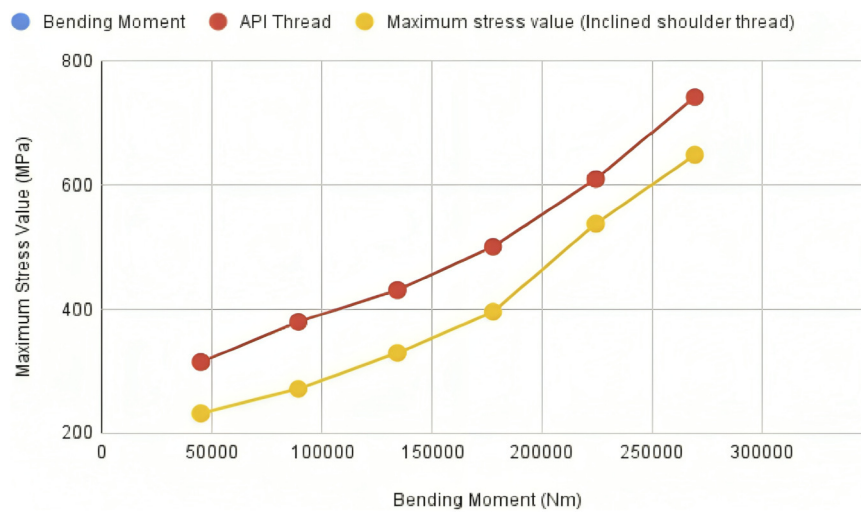


FIGURE 6 Comparison of Maximum Mises stress values at various bending moments (Reproduced from Zhu, 2016).

deformation hot rolling method was applied. The findings demonstrated that this redesigned drill pipe steel completely complies with the “leak-before-break” fracture concept, having a yield strength of 150 ksi and an impact toughness of more than 150 J. Conventional drill pipes are made of High-strength low-alloy steels (HSLA) and are reinforced using a process that combines grain refining, solid-solution strengthening, dislocation strengthening, and precipitation hardening (Dong et al., 2017). In recent decades, HSLA steels infused with Mo, V, Ni, and other elements have gained supremacy in drill pipe applications. These steels have yield strengths of 400–500 MPa. Precipitation hardening was originally thought to have little impact on these values since many alloying elements were mixed with HSLA steels to improve grain refinement. Grain refinement, which is the major way to enhance toughness while increasing strength, is the key approach for strengthening drill pipe steel (Hu et al., 2011). Toughness could be boosted by adding an alloying element. First, the addition of any alloying element causes the microstructure to change, mostly through changing the hardenability, phase transition temperature, precipitation morphology, and grade of grain. Additionally, the presence of an alloying metal like Ni encourages matrix cross-slip deformation. The distribution of fine carbides must be uniform, and the number of coarse carbides must be reduced. These requirements may be managed by the design of the alloy, production procedure, and the treatment through heat.

3.7 Analysis of drill pipe failures due to galling

Spectroscopic chemical analysis can be used to determine the chemical composition of tool joints (Li et al., 2013). Optically assisted metallography was used to observe microstructure at different locations. By using scanning electron microscopy and ocular inspection, the galling surface was observed (SEM). Galling can be avoided with ease and effectiveness by coating threads with ion-plated films (White, 1984). According to a

study by Li et al. (2013), the metallographic analysis result suggests that there has been structural degradation in the tool joints’ outer surface. Initiation of mini-cracks has also come from the white bright layer. Micro-surface examination reveals that the guiding surface of the threads was spalled in some areas and suffered more severe damage than the bearing surface. Microscopic and macroscopic investigations revealed that the guiding surface of the damaged thread was more severely damaged than the bearing surface and was typically inclined towards the bearing surface. It has been hypothesized that the make-up process resulted in thread-galling failure. Plough traces and transition of metal were created on the profile of the thread along with the relative sliding of the rotary-shouldered thread connection. Metal deposition will cause the thread connection, which is rotary shouldered, to gall and fail. The findings of the test, microstructure, and conditions of the field led to the conclusion that the cause of galling failure may be related to the material’s performance. To control and lower the same galling failure incidents, quality inspection must be strengthened, and activities must be strictly regulated (Li et al., 2013).

3.8 Analysis of drill pipe failures due to axial forces

A computational and experimental investigation by Duman et al. (2003), on the influence of the tool joints on axial force transmission, concluded that the introduction of tool joints increased the critical buckling load by up to 20%, while enhancing the axial load transfer efficiency by about 40%. Axial tensile stress is regarded as the primary factor in the simulation carried out by Li et al. (2011), based on the structure of the drill pipe. The transition zone is much more stressed than other areas of the pipe and joint when subjected to the effects of an axial tensile load. The transitional zone’s round corner is where stress concentration is at its highest level.

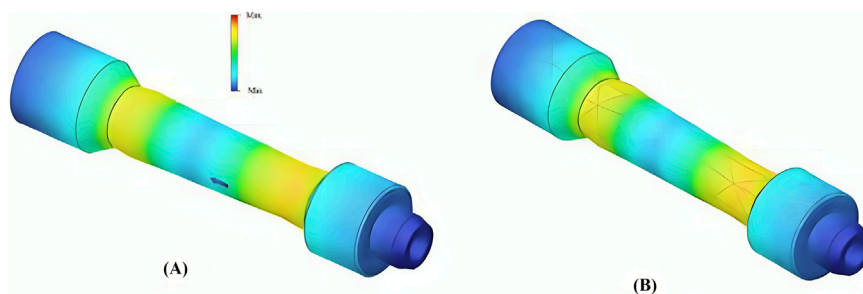


FIGURE 7 Drill pipe made of aluminum under the given loads. (A) Diagram which shows scheme of design; (B) Strained condition caused by torsion and compression; 1 – Drill pipe made of aluminum which has protector thickening; 2 – The well wall (Reproduced from Vlasiy et al., 2017).

The fillet radius of curvature between the zone of transition and the tube pipe is the most problematic place, according to a simulation study, where the stress concentration is noticeably more than in other drill pipe and tool joint zones. The transition zone appears to be the drill pipe’s weak point based on the stress distribution. The main region where washout or fracture takes place is the transition zone. According to statistics, that site accounted for 85% of drill pipe failures.

3.9 Analysis of drill pipe failures due to torque

A mathematical modeling was performed by Vlasiy et al. (2017), to analyze the effect of torque to determine the stability of the pipe. According to this model, the O_{xyz} coordinate system is employed, with the hanging point serving as the coordinate system’s origin (Figure 7).

The drill pipe’s axial line and the O_x axis are parallel. O_y and O_z axes are chosen as the primary axes of cross-sectional inertia. The axial directions divide the torque into the parts, M_y' and M_z' . Moments are P_y and P_z , which are explained in Equations 12, 13:

$$-E * I(x) * z'' = P * z - M * y' \tag{12}$$

$$-E * I(x) * y'' = P * y + M * z' \tag{13}$$

where E refers to the Young’s modulus of elasticity (Pa), $I(x)$ refer to the pipe’s cross-sectional moment of inertia with abscissa at the point x ($kg \cdot m^2$).

Boundary conditions, used to analyze the differential equation system, are $z'(0) = y(0) - z(0) = 0, y'(L) = z'(L) = 0$.

The bending rigidity of the drill pipe is detailed by a single analytical expression in the form of Equation 14:

$$EI(x) = \sum_{k=0}^4 EI_k(x) \Theta_k(x), k = 0, \tag{14}$$

where $I_k(x)$ refers to the pipe’s cross-sectional moment of inertia in element x ($kg \cdot m^2$):

$$X \in [x_k; x_{k+1}), \Theta_k(x) = \begin{cases} 1, & x \in [x_k; X_{k+1}) \\ 0, & x \notin [x_k; X_{k+1}) \end{cases}$$

According to Equation 15 the cross-section of aluminum drill pipe (ADP) takes a ring form:

$$I_k(x) = \frac{E\pi D_k^4(x)}{64} \left[1 - \left(\frac{dk(x)}{Dk(x)} \right)^4 \right], k = \overline{0, 4}, \tag{15}$$

Here, $k = 0, 1, 2, 3, 4$.

Where $d_k(x), D_k(x)$ refer to the drill pipe’s interior and exterior diameters in the element, respectively. The introduction of a 2D vector $V(x) = (z(x), y(x))^T$, along with the second-order square matrices, reduces this Equation 16 to the first-order differential system.

$$A(x) = (EI(x))J, B(x) = (EI(x)) - 1E2, \tag{16}$$

where $(EI(x))^{-1} = \sum_{k=0}^4 (EI(x))^{-1} \Theta_k(x), J = \begin{pmatrix} 0 & -1 \\ 1 & 0 \end{pmatrix}, E_2 = \begin{pmatrix} 1 & 0 \\ 0 & 1 \end{pmatrix}$.

Followed by 4D vector $U(x) = (V(x), V'(x))^T$ and square matrix with an order of 4 in Equation 17:

$$C(x) = \begin{pmatrix} O_2 & E_2 \\ -PB(x) & -MA(x) \end{pmatrix}, \tag{17}$$

where O_2 refers to the second-order zero matrix.

$U(x) = K(x, P, M)C$ is the general solution of the obtained boundary problem, where C refers to the arbitrary sustained 4D vector and $K(x, P, M)$ refers to the basic Cauchy matrix system of the fourth order, normalized by the rule $K(0, P, M) = E_2$.

$\Delta(P, M) \equiv \det [R + SK(l, P, M)] = 0$ is the determinant.

Where R and S refer to the boundary matrices as shown in Equation 18:

$$R = \begin{pmatrix} E_2 & E_2 \\ O_2 & O_2 \end{pmatrix}, S = \begin{pmatrix} O_2 & O_2 \\ O_2 & E_2 \end{pmatrix} \tag{18}$$

The main portion of the pipe is divided into equal segments (n), each measuring $h = 1/n$ in length. A characteristic determinant is obtained and shown in Equation 19:

$$\Delta_n(P, M) = \det \left[R + S \prod_{k=0}^{n-1} \begin{pmatrix} E_2 & -\frac{h}{Mc_{n-k}} J [E - e^{-Mc_{n-k}J}] \\ -Pc_{n-k}E_2 & -\frac{Ph}{M} J [E - e^{-Mc_{n-k}J}] + e^{-Mc_{n-k}J} \end{pmatrix} \right] \tag{19}$$

where $c_k = \int_{\epsilon_k}^{\epsilon_{k+1}} (EI(x))^{-1} dx$.

By setting the values of axial force P , the critical values of Torque M can be calculated using Equations 20, 21.

According to (Samuel, 2011).

The torque is given by,

$$T = F_a \times \frac{d}{2} = \mu r F_s \quad (20)$$

When the pipe is reciprocated and rotated,

$$T = \mu \times F_s \times r \times \frac{|\omega|}{|V_{rs}|} \quad (21)$$

where $|V_{ts}|$ refers to the trip speed at which the tripping operation is carried out, $|V_{rs}|$ refers to the resultant speed ($\sqrt{V_{ts}^2 + \omega^2}$), $|\omega|$ refers to angular speed (diameter $\times \pi \times \frac{RPM}{60}$), F_s refers to the side or normal force, μ refers to the Coefficient of friction, R refers to the Component radius.

The equilibrium angle torque can be calculated using Equation 22:

$$T = \frac{\mu_v}{\sqrt{1 + \mu_v^2}} \times F_s \times r \times \frac{|\omega|}{|V_{rs}|} \quad (22)$$

where the varying friction coefficient is calculated using Equation 23:

$$\mu_v = \mu_s \times e^{-k|V_{rs}|} \quad (23)$$

where k refers to speed constant.

Over-torque can result in drill pipe thread damage, and the solution is to consistently tighten the pipe connections to their ideal levels. To establish the ideal make-up torque, mathematical modeling is required.

3.10 Analysis of drill pipe failures due to torsional vibration

Researchers are very concerned with finding ways to reduce drill string torsional vibrations. One objective is to increase the operating speed range, where the drill bit may whirl in the absence of triggering limit cycles, in which the bit sticks, the drill string twists, and elastic potential energy is stored. The energy, which is obtained, is then converted into kinetic energy when it exceeds the opposing friction forces. The bit may pick up speed and increase its angular velocity by a factor of several orders of magnitude. The second objective is to develop reliable control systems that might not need a lot of on-site tuning for various drill string setups or tuning because drilling conditions change. Although researchers have proposed methods, they have not come up with solutions.

3.11 Analysis of drill pipe failures due to axial vibration

The approach that reduces drill stem resonance is presented once the mechanical regulations of the drill stem have been studied to find the fundamental rule of the system of the drill stem (Booman et al., 2013). Using Delphi software, it is possible to determine the eigenfrequency of the drill stem vibration axially. Although the frequency may reach extremely high values, they are not within the scope of the real drilling scenario; thus, we may not take them into account. Several frequencies are close to the drilling condition in reality, and the frequency rises as the number of steps rises. The rotary table revolves at 54 rpm when a three-tooth bit is employed, and the system may be in an extremely risky condition of resonance.

Due to this, the rotary table's speed is 55 rpm, which is not an acceptable parameter for the frequency of 2.705 Hz. After guaranteeing the safety of the drill stem, the rotary table's speed should be much higher (Chunjie and Tie, 2009).

The rotary table's speed is acceptable because the initial resonant frequency zone is focused on a frequency that is distant from this value. This frequency is determined by the axial vibration of the string, which is stronger than in other resonance scenarios. Delphi allows for the display of the procedure's results. The modification of the drilling conditions allows for modification of the drilling parameter. The frequency at which the rotary table should operate depends on maximum axial and radial loads. In most cases, for a specific well, the drill pipe length remains the same as the well depth changes. The drill stem acts like a cord with a soft texture, while the well depth increases and exhibits very complex dynamic behavior. The system's substantial axial vibrations have a significant impact that is not negligible. Delphi analyzes the circumstance where the frequency of a drill stem's vibration axially varies with the well depth (Chunjie and Tie, 2009).

3.12 Analysis of drill pipe failure due to wear and corrosion

Due to their tiny grains and high interfacial density, nanocrystalline materials exhibit good friction and corrosion resistance, as well as high hardness and strength (Lu, 1996). The creation of the nanocrystalline layer might be a useful technique for increasing the corrosion resistance and wear resistance of drill pipes made of aluminum alloy. Several important grain-refining techniques, such as supersonic fine particle bombardment (Han et al., 2012), laser shock processing (Cui et al., 2014; Dai et al., 2012), surface mechanical attrition treatment (Wen et al., 2011; Lei et al., 2015), and Ultrasonic Cold Forging Technology (Gu et al., 2016), are used to create nanocrystalline materials. The creation of a nanostructured surface layer using the UCFT is a relatively new technique that is easier to use and environmentally beneficial. Surface engineering techniques, such as surface nano crystallization (Liang et al., 2018; Wen et al., 2011; Gu et al., 2016; Ahn et al., 2012; Chen et al., 2014; Liu et al., 2018; Tian et al., 2002), and micro-arc oxidation (Tang et al., 2011; Yi et al., 2018; Chen et al., 2013; Ding et al., 2010; Li et al., 2014), can enhance the corrosion wear resistance of aluminum alloy drill pipes.

In Liang et al. (2018), Micro-arc oxidation (MAO) with ultrasonic cold forging technology (UCFT) was used to treat the 2,618 aluminum alloy, producing a strengthening coating. This enhanced the ability of drill pipes made of aluminum alloy to withstand corrosion and wear in use for geological and petroleum drilling (MAO). The UCFT refined the aluminum alloy grain, producing nanostructured grains. Corrosion made the wear worse in the drilling fluid environment. The samples of MAO and UCFT + MAO wear rates were less after 720 h of corroding in the drilling fluid, and there was more corrosion inhibition than there was in the case of the untreated sample. Both the UCFT sample's and the untreated sample's layers of corrosion developed numerous microcracks, which hastened the wear. The surface MAO layers on the MAO and UCFT + MAO specimens were mostly unaffected, not corroding the interior coating or creating microcracks, showing that these samples had

significantly higher corrosion-wear resistance. Wear is prevented by the UCFT + MAO sample's exceptional hardness. Following cold forging using an ultrasound procedure, the aluminum alloy's surface grain was fine-tuned, and a much smaller MAO coating with a reliable plasma channel was produced in the MAO process. As a result, this sample demonstrated higher resistance to corrosion and wear. The outcomes showed that the MAO and UCFT methods increased the aluminum alloy's corrosion and wear resistance, particularly its resistance to salt corrosion (Ali et al., 2020; Liang et al., 2018).

A wear-resistant protective metal covering known as "hard banding" is applied by electric welding to the drill pipe and the pipe joint's exterior (Fedorova et al., 2020). By coating the drill pipe, collars, and drill pipe tool joints with a layer of very hard metal, the drill stem and casing components are both protected from drilling-related wear. To be able to shield expensive drill stem equipment from damage caused by axial and rotating forces while tripping and drilling in and out of a well, drilling contractors and operators needed strong banding decades ago.

Since the late 1930s, the drill pipe tool joints and other equipment used in drilling have been hard-banded (Barrios et al., 2002; Mobley, 1999). Hard banding was initially used mainly to prevent early abrasive wear on the drill pipe and other instruments. Since then, hard banding and its use have undergone a number of alterations, but only recently has advanced technology been developed that enables hard banding to simultaneously protect the casing and the drill pipe. For hard banding, a variety of wear-resistant alloy types are now accessible. The majority of the alloy types are made to safeguard the casing, the marine riser, or the drill pipe, but only one or two can effectively prevent early abrasive wear. With the right application, hard banding can significantly extend the lifespan of drill pipes and tool joints, reduce downhole drag and torque, and rig fuel consumption, as well as enabling operators to run casing that is lighter in weight and of higher quality (Murthy et al., 2011). It was advised to improve the arrangement in the inner upset-taper, employ internally coated drill pipes, and upgrade the standard of the pipe's construction materials (Lu et al., 2005).

4 Summary

For each of the projected failures in drill pipes during horizontal directional drilling, several numerical analyses were conducted. The findings from the analysis of drill pipe failures due to various factors are listed below:

- SEM, Ocular examination, as well as optical microscopy, were used to evaluate the fracture surface in the instance of decarburization to determine the types of cracks formed. A seamless tubular hot rolling method was performed to enhance the materials' mechanical characteristics, drill pipe body, and reduce high residual tensile stress. The main reason for the decarburization layer on the exterior of the drill pipe is due to improper heat treatment.
- Generalized likelihood ratio test (GLRT) is utilized to identify changes due to drill pipe washout failures. GLRT uses the noise distribution along with estimating a set of friction characteristics. In addition, early detection is another outcome that can be used to solve this problem.
- The drill pipe's fatigue life is determined using the Palmgren-Miner Linear Damage Summation Rule. The stress-life (S-N) method, the Strain-life method, and the Linear elastic fracture mechanics (LEFM) method are the three fatigue failure models that are analyzed in this case. It is also found that the pipe joint is the weakest point in the pipe.
- In the case of drill pipe failures due to grain boundaries, microstructure refinement is a cost-effective and efficient way of resolving the issue. The Hall-Petch relationship gives the result that tensile strength improves as grain size decreases. Furthermore, grain refining can improve the strength and toughness of materials.
- Analysis of drill pipe failures due to bending moment is done by comparing a 3D Finite Element Model (FEM) and experimental values of Mises stress distribution of the finite element calculation. It is found that both results coincide. The improvements, based on these observations, found were an angled shoulder thread, suitable for withstanding a greater bending moment. As a consequence of this, a higher bending yield strength is present in the inclined shoulder thread.
- To tackle the problems faced by drill pipe failures due to fracture and piercement, drill pipes made of HSLA steels are used. These steels were alloyed to increase the grain refining, which further increases the strength of the drill pipe, thus solving the problem.
- Initial procedure for solving the drill pipe failures due to galling is to observe the galling surface using scanning electron microscopy and ocular inspection. A galling problem can be avoided with ease and effectiveness by coating threads with ion-plated films.
- A mathematical model was deduced to predict the ideal make-up torque as a solution to avoid drill Pipe Failures due to torque.
- Analysis of drill pipe failures due to torsional vibrations - Further research is needed to shed light on these issues.
- Delphi software is used to establish the natural frequency of the drill string's axial vibration. Delphi allows for the display of the procedure's results. The modification of the drilling conditions allows for the modification of the drilling parameter. With the help of this software, the problem of drill pipe failure due to axial vibration can be tackled.
- The corrosion, as well as wear resistance, of aluminum alloy drill pipes, were improved using the ultrasonic cold forging technology (UCFT) and micro-arc oxidation (MAO). Therefore, UCFT technology and MAO technology increased the aluminum alloy's corrosion and wear resistance, particularly its resistance to salt corrosion.

Study of a pipe-scanning robot for use in horizontal drilling's post-construction evaluation, AI machine learning, Big data, Sensor Analytics are some of the examples that have a great scope of research for improving studies done in this field.

Through the twelve mechanisms re-examined, fatigue and vibration-induced failures arise as reported in HDD operations.

Upcoming research could focus on coupled modelling of fatigue and vibration, real-time monitoring of drill pipe stresses, and

development of predictive maintenance strategies to mitigate HDD failures.

Author contributions

HR: Data curation, Formal Analysis, Investigation, Methodology, Resources, Software, Validation, Visualization, Writing – review and editing. AM: Conceptualization, Writing – original draft, Writing – review and editing.

Funding

The author(s) declared that financial support was not received for this work and/or its publication.

Acknowledgements

The authors are thankful to Kappa, Fusion 360, and AutoCAD software for providing Academic Licensed Software to perform the research. We thank the administration of Vellore Institute of Technology for providing all the necessary facilities. We would also like to thank Shaun M. Varghese for illustrating drill pipes in Fusion 360 software.

References

- Ahn, D., He, Y., Wan, Z., Cho, I. S., Lee, C. S., Park, I. G., et al. (2012). Effect of ultrasonic nano-crystalline surface modification on the microstructural evolution and mechanical properties of Al5052 alloy. *Surf. Interface Analysis* 44 (11–12), 1415–1417. doi:10.1002/sia.4959
- Ali, J. A., Kalthury, A. M., Sabir, A. N., Ahmed, R. N., Ali, N. H., and Abdullah, D. A. (2020). A state-of-the-art review of the application of nanotechnology in the oil and gas industry with a focus on drilling engineering. *J. Petroleum Sci. Eng.* 191 (August), 107118. doi:10.1016/j.petrol.2020.107118
- Barrios, J., Alonso, C., Pedersen, E., Bachelot, A., and Broucke, A. (2002). “Hardbanding for drilling unconsolidated sand reservoirs,” in *IADC/SPE Asia Pacific drilling technology, September 9, SPE-77246-MS*. doi:10.2118/77246-MS
- Baryshnikov, A., Calderoni, A., Ligrone, A., and Ferrara, P. (1997). A new approach to the analysis of drillstring fatigue behavior. *SPE Drill. and Complet.* 12 (02), 77–84. doi:10.2118/30524-PA
- Bert, D. R., Storaune, A., and Zheng, N. (2009). Case study: drillstring failure analysis and new deep-well guidelines lead to success. *SPE Drill. and Complet.* 24 (04), 508–517. doi:10.2118/110708-PA
- Booman, J., Kunert, H., and Otegui, J. L. (2013). Loss of a 30" directional crossing due to pipeline collapse during pullback. *Eng. Fail. Anal.* 33 (October), 388–397. doi:10.1016/j.engfailanal.2013.06.001
- Cao, M. (2011). Research on fatigue mechanism and fatigue life of drill pipes used in horizontal directional drilling. *ICPTT* 7, 912–917. doi:10.1061/41202(423)96
- Cao, J., Yong, Q., Liu, Q., and Sun, X. (2007). Precipitation of MC phase and precipitation strengthening in hot rolled Nb–Mo and Nb–Ti steels. *J. Mater. Sci.* 42 (24), 10080–10084. doi:10.1007/s10853-007-2000-4
- Cao, M., Shi, Z.-J., and Tian, D.-Z. (2009). Influence of space between hole and pipes on drill pipes' failure. *ICPTT* 15, 2069–2074. doi:10.1061/41073(361)219
- Charleux, M., Poole, W. J., Militzer, M., and Deschamps, A. (2001). Precipitation behavior and its effect on strengthening of an HSLA-Nb/Ti steel. *Metallurgical Mater. Trans. A* 32 (7), 1635–1647. doi:10.1007/s11661-001-0142-6
- Chehab, A. G., and Moore, I. (2010). Pipe-soil shear interaction stiffness in horizontal directional drilling and pipe bursting. *Geomechanics Geoengin.* 5 (2), 69–77. doi:10.1080/17486020903497449
- Chen, C. Y., Yen, H. W., Kao, F. H., Li, W., Huang, C., Yang, J., et al. (2009). Precipitation hardening of high-strength low-alloy steels by nanometer-sized carbides. *Mater. Sci. Eng. A* 499 (1–2), 162–166. doi:10.1016/j.msea.2007.11.110

Conflict of interest

The author(s) declared that this work was conducted in the absence of any commercial or financial relationships that could be construed as a potential conflict of interest.

Generative AI statement

The author(s) declared that generative AI was not used in the creation of this manuscript.

Any alternative text (alt text) provided alongside figures in this article has been generated by Frontiers with the support of artificial intelligence and reasonable efforts have been made to ensure accuracy, including review by the authors wherever possible. If you identify any issues, please contact us.

Publisher's note

All claims expressed in this article are solely those of the authors and do not necessarily represent those of their affiliated organizations, or those of the publisher, the editors and the reviewers. Any product that may be evaluated in this article, or claim that may be made by its manufacturer, is not guaranteed or endorsed by the publisher.

- Chen, M., Liu, S.-Y., Li, J.-M., Cheng, N., and Zhang, X.-M. (2013). Improvement to corrosion resistance of MAO coated 2519 aluminum alloy by formation of polypropylene film on its surface. *Surf. Coatings Technol.* 232 (October), 674–679. doi:10.1016/j.surfcoat.2013.06.073

- Chen, B., Huang, B., Liu, H., Li, X., Ni, M., and Chen, Lu (2014). Surface nanocrystallization induced by shot peening and its effect on corrosion resistance of 6061 aluminum alloy. *J. Mater. Res.* 29 (24), 3002–3010. doi:10.1557/jmr.2014.323

- Chunji, H., and Tie, Y. (2009). “The research on axial vibration of drill string with Delphi,” *2009 International Conference on Computational Intelligence and Natural Computing*, June, 478–481. doi:10.1109/CINC.2009.85

- Cocciolo, P. P., and Zeleny, B. (2004). “Risk reduction measures applied to horizontal directional drilling of a complex pipeline river crossing in Canada.” *Int. Pipeline Conf.* (1-3), 459–466. doi:10.1115/IPC2004-0069

- Cui, C. Y., Cui, X. G., Zhao, Q., Ren, X., Zhou, J., Liu, Z., et al. (2014). Simulation, microstructure and microhardness of the Nano-SiC coating formed on Al surface via laser shock processing. *Mater. and Des.* 62, 217–224. doi:10.1016/j.matdes.2014.05.027

- Dai, F. Z., Lu, J. Z., Zhang, Y. K., Luo, K., Wang, Q., Zhang, L., et al. (2012). Effect of initial surface topography on the surface status of LY2 aluminum alloy treated by laser shock processing. *Vacuum* 86 (10), 1482–1487. doi:10.1016/j.vacuum.2012.02.001

- Dale, B. A. (1988). An experimental investigation of fatigue-crack growth in drillstring tubulars. *SPE Drill. Eng.* 3 (04), 356–362. doi:10.2118/15559-PA

- Ding, H.-yan, Dai, Z.-dong, Skuiry, S. C., and Hui, D. (2010). Corrosion wear behaviors of micro-arc oxidation coating of Al₂O₃ on 2024Al in different aqueous environments at fretting contact. *Tribol. Int.* 43 (5–6), 868–875. doi:10.1016/j.triboint.2009.12.022

- Dong, Ji, Liu, C., Liu, Y., Zhou, X., Guo, Q., and Li, H. (2017). Isochronal phase transformation of nb–v–ti microalloyed ultra-high strength steel upon cooling. *Fusion Eng. Des.* 125 (December), 423–430. doi:10.1016/j.fusengdes.2017.05.025

- Duman, O. B., Miska, S., and Kuru, E. (2003). Effect of tool joints on contact force and axial-force transfer in horizontal wellbores. *SPE Drill. and Complet.* 18 (03), 267–274. doi:10.2118/85775-PA

- Fangpo, Li, Yonggang, L., and Lu, C. (2011). “Failure analysis of 127mm G105 drill pipe,” in *2011 International Conference on Materials for Renewable Energy and Environment*, May, 1813–1816. doi:10.1109/ICMREE.2011.5930687

- Fedorova, L., Fedorov, S., Ivanova, Y., Voronina, M., Fomina, L., and Morozov, A. (2020). Improving drill pipe durability by wear-resistant surfacing. *Mater. Today Proc.* 30, 398–403. doi:10.1016/j.matpr.2019.12.384

- Gu, Y., Chen, L., Wen, Y., Chen, P., Chen, F., and Ning, C. (2016). Corrosion behavior and mechanism of MAO coated Ti6Al4V with a grain-fined surface layer. *J. Alloys Compd.* 664 (April), 770–776. doi:10.1016/j.jallcom.2015.12.108
- Guang-sheng, WANG, and Hong, S. (2007). *Defect analysis in metal heat treatment*. Beijing: Mechanical Industry Press.
- Gwilliam, Mr W. J. (1999). Implement Russian aluminum drill pipe and retractable drilling bits into the USA.
- Han, Y.-jun, Ye, F.-xing, Ding, K.-ying, Wang, Z.-ping, and Lu, G.-xiong (2012). Effects of supersonic fine particles bombarding on thermal barrier coatings after isothermal oxidation. *Trans. Nonferrous Metals Soc. China* 22 (7), 1629–1637. doi:10.1016/S1003-6326(11)61366-6
- Hansford, J. E., and Lubinski, A. (1966). Cumulative fatigue damage of drill pipe in dog-legs. *J. Petroleum Technol.* 18 (03), 359–363. doi:10.2118/1258-PA
- Hawkins, D. E. (2005). *The bending moment*. Palgrave Macmillan UK. doi:10.1057/9780230510609
- Hu, F., Han, Li H., Wang, H., Feng, Y. R., and Li, He L. (2011). The development and experimental study on high strength and toughness drill pipe steel. *Adv. Mater. Res.* 287–290 (July), 1024–1032. doi:10.4028/www.scientific.net/AMR.287-290.1024
- Jacoby, G. (1966). Application of microfractography to the study of crack propagation under fatigue stresses.
- Lee, W.-B., Hong, S.-G., Park, C.-G., and Park, S.-Ho (2002). Carbide precipitation and high-temperature strength of hot-rolled high-strength, low-alloy steels containing Nb and Mo. *Metallurgical Mater. Trans. A* 33 (6), 1689–1698. doi:10.1007/s11661-002-0178-2
- Lei, W., Yuan, Y., Wang, Y., and Ying, J. (2015). Effect of nanocrystalline surface and iron-containing layer obtained by SMAT on tribological properties of 2024 Al alloy. *Rare Metal Mater. Eng.* 44 (6), 1320–1325. doi:10.1016/S1875-5372(15)30082-5
- Li, F., and Wang, Y. (2015). Effect of surface decarburization on S135 drill pipe's service property. 40 (July): 164–167. doi:10.13251/j.issn.0254-6051.2015.07.039
- Li, F.Po, Liu, Y. G., and Yong, W. (2011). Piecing failure analysis of drill pipe upset. *Adv. Mater. Res.* 314–316 (August), 1210–1213. doi:10.4028/www.scientific.net/AMR.314-316.1210
- Li, F., Liu, Y., and Chen, W. (2013). Galling failure analysis of drill pipe rotary-shouldered thread connections for horizontal directional drilling. *ICPTT*, 452–460. doi:10.1061/9780784413142.048
- Li, C.-yang, Liu, D.-xin, and Ye, Z.-yan (2014). Effect of the micro-arc oxidation and cerium salt sealing on the corrosion and wear resistance of new 7A85. *Mech. Sci. and Technol. Aeronaut. Eng.* 33 (1), 127–132.
- Li, L., Lian, Z., and Zhou, C. (2022). Failure analysis of drill pipe during working process in a deep well: a case study. *Processes* 10 (9), 1765. doi:10.3390/pr10091765
- Lian, Z., Chen, D., Wei, W., Zhou, Y., and Jiang, J. (2014a). Corrosion analysis of G105 coating drill-pipe washout. *Anti-Corrosion Methods Mater.* 61 (6), 365–369. doi:10.1108/ACMM-04-2013-1250
- Lian, Z., Chen, D., Wei, W., Zhou, Y., and Jiang, J. (2014b). Corrosion analysis of G105-Coated drill-pipe washout and electroless plating Ni-P as drill-pipe protection in freshwater mud. *Corrosion* 70 (6), 652–659. doi:10.5006/1040
- Liang, J., Wen, Y., Gu, Y., Liu, J., Wang, C., and Ma, H. (2018). Improving corrosion resistance and corrosive wear resistance of aluminum alloy drill pipe by surface nanocrystallization and micro-arc oxidation. *J. Mater. Eng. Perform.* 27 (9), 4462–4472. doi:10.1007/s11665-018-3529-x
- Liu, W.-Y., Shi, T.-H., Zeng, D.-Z., Zhu, Z. H., Jia, H. M., Lu, Q., et al. (2011). Study on drill pipe with mud membrane corrosion mechanics under atmospheric environment. *J. Mater. Eng.* 1 (8), 19–23.
- Liu, J., Wen, Y., Liang, J., Hou, B., Sun, J., She, D., et al. (2018). Effects of evaluated temperature on tribological behaviors of micro-arc oxidized 2219 aluminum alloy and their field application. *Int. J. Adv. Manuf. Technol.* 96 (5–8), 1725–1740. doi:10.1007/s00170-017-0919-4
- Lu, K. (1996). Nanocrystalline metals crystallized from amorphous solids: nanocrystallization, structure, and properties. *Mater. Sci. Eng. R Rep.* 16 (4), 161–221. doi:10.1016/0927-796X(95)00187-5
- Lu, S., Feng, Y., Luo, F., Qin, C., and Wang, X. (2005). Failure analysis of IEU drill pipe wash out. *Int. J. Fatigue* 27 (10–12), 1360–1365. doi:10.1016/j.ijfatigue.2005.07.012
- Lu, C., Liu, Y., Wang, X., Jun, W. G., and Song, S. (2011). Failure analysis of horizontal directional drilling crossing drill pipe fracture. *ICPTT* 7, 958–964. doi:10.1061/41202(423)101
- Lv, S. L., Luo, F. Q., Zhou, J., Liu, Y. Y., Su, J. W., and Lu, Q. (2009). Analysis on Applicat-Ion prospect of aluminum alloy drill pipe in tarim oilfield. *Pet. Drill. Tech.* 37, 74–77.
- Ma, F. (2004). *Fatigue of drill pipes used in horizontal directional drilling*. Ruston: Louisiana Tech University.
- Ma, F., Sterling, R., and Allouche, E. (2005). Fatigue of drill pipes used in mini-horizontal directional drilling. *Pipelines* 19, 1–15. doi:10.1061/40800(180)1
- Macdonald, K. A., and Bjune, J. V. (2007). Failure analysis of drillstrings. *Eng. Fail. Anal.* 14 (8), 1641–1666. doi:10.1016/j.engfailanal.2006.11.073
- Machado, C. R., Rizzi, J., Xavier, C., Rocha, L. D. B., Souza, L. O., Ferreira, P., et al. (2022). "Development of drill pipes failure prediction models and operational management system using real-time data analytics and Ai." in *IADC/SPE Asia Pacific drilling technology conference and exhibition*, D021S006R001. doi:10.2118/209858-MS
- Mao, W. M., Zhu, J. C., Li, J., Long, Yi, and Fan, Q. C. (2008). The structure and properties of metallic materials.
- Mobley, J. G. (1999). Hardbanding and its role in deepwater drilling. *SPE/IADC Drill. Conf. March 9*, SPE-52882-MS. doi:10.2118/52882-MS
- Murthy, G. V. S., Das, G., Kumar Das, S., Parveen, N., and Singh, S. R. (2011). Hardbanding failure in a heavy weight drill pipe. *Eng. Fail. Anal.* 18 (5), 1395–1402. doi:10.1016/j.engfailanal.2011.03.014
- National Research Technological University, Komissarov, A. A., Ozherelkov, D. Yu., et al. (2020). Causes of high-strength drill pipes failure. *Deformation Fract. Mater.* 10, 29–33. doi:10.31044/1814-4632-2020-10-29-33
- Polak, M. A., and Lasheen, A. (2001). Mechanical modelling for pipes in horizontal directional drilling. *Tunn. Undergr. Space Technol.* 16 (January), 47–55. doi:10.1016/S0886-7798(02)00020-2
- Rahman, M. (1999). Stress concentration incorporated fatigue analysis of die-marked drill pipes. *Int. J. Fatigue* 21 (8), 799–811. doi:10.1016/S0142-1123(99)00039-0
- Rahman, M. K., Hossain, M. M., and Rahman, S. S. (1999). Survival assessment of die-marked drill pipes. *Eng. Fail. Anal.* 6 (5), 277–299. doi:10.1016/S1350-6307(98)00052-1
- Samuel, R. (2011). *Formulas and calculations for drilling operations*, 50. John Wiley and Sons.
- Sikal, A., Gilbert Boulet, J., Menand, S., and Sellami, H. (2008). Drillpipe stress distribution and cumulative fatigue analysis in complex well drilling: new approach in fatigue optimization. *All Days, Sept. 21*, SPE-116029-MS. doi:10.2118/116029-MS
- Simpson, B., Payne, M. L., Jellison, M. J., and Adams, B. A. (2004). 2,000,000 lb. Landing string developments: novel slips technology extends the deepwater operating envelope. *IADC/SPE Drill. Conf. March 2*, SPE-87186-MS. doi:10.2118/87186-MS
- Sun, J. H., Liang, J., and Zhang, Y. Q. (2011). Development of high-strength aluminum alloy drill rod and its application in geological drilling. *Explor. Eng.* 1, 48.
- Sun, Y., Peng, X., and Bi, G. (2024). Study on S-N curve and fatigue limit of drill pipe in offshore short-radius sidetracking process. *Processes* 12 (9), 1828. doi:10.3390/pr12091828
- Tang, Y., Xu, J. Y., Ye, F. Y., Gao, C., Zhang, J. C., and Liu, Ya J. (2011). Antiwear behavior of micro-arc oxidated coating rubbing on abrasive paper. *Mater. Sci. Forum* 704-705 (December), 704–705. doi:10.4028/www.scientific.net/MSF.704-705.1210
- Tian, J., Luo, Z., Qi, S., and Sun, X. (2002). Structure and antiwear behavior of micro-arc oxidized coatings on aluminum alloy. *Surf. Coatings Technol.* 154 (1), 1–7. doi:10.1016/S0257-8972(01)01671-1
- Ullah, F. K., Duarte, F., and Bohn, C. (2016). A novel backstepping approach for the attenuation of torsional oscillations in drill strings. *Solid State Phenom.* 248 (March), 85–92. doi:10.4028/www.scientific.net/ssp.248.85
- Van Swygenhoven, H. (2002). Grain boundaries and dislocations. *Science* 296 (5565), 66–67. doi:10.1126/science.1071040
- Varma, S. K., and Vasquez, G. (2003). Corrosive wear behavior of 7075 aluminum alloy and its composite containing Al₂O₃ particles. *J. Mater. Eng. Perform.* 12 (1), 99–105. doi:10.1361/105994903770343547
- Velikov, K. P., Christova, C. G., Dullens, R. P. A., and Van Blaaderen, A. (2002). Layer-by-Layer growth of binary colloidal crystals. *Science* 296 (5565), 106–109. doi:10.1126/science.1067141
- Vlasiy, O., Mazurenko, V., Ropyak, L., and Rogal, O. (2017). Improving the aluminum drill pipes stability by optimizing the shape of protector thickening. *Восточно-Европейский Журнал Передовых Технологий* 1 (7), 25–31. doi:10.15587/1729-4061.2017.65718
- Voort, G. F. V. (2015). Understanding and measuring decarburization. *AM&P Tech. Artic.* 173 (2), 22–27. doi:10.31399/asm.amp.2015-02.p022
- Wen, L., Wang, Y., Zhou, Yu, Guo, L., and Ouyang, J.-Hu (2011). Microstructure and corrosion resistance of modified 2024 Al alloy using surface mechanical attrition treatment combined with microarc oxidation process. *Corros. Sci.* 53 (1), 473–480. doi:10.1016/j.corsci.2010.09.061
- White, G. W. (1984). Eliminating galling of high-alloy tubular threads by high-energy ion deposition process. *J. Petroleum Technol.* 36 (08), 1345–1351. doi:10.2118/12209-PA

- Willersrud, A., Blanke, M., Imsland, L., and Pavlov, A. (2015). Drillstring washout diagnosis using friction estimation and statistical change detection. *IEEE Trans. Control Syst. Technol.* 23 (5), 1886–1900. doi:10.1109/TCST.2015.2394243
- Xu, X., Yin Song, S., Feng, Y. R., and Wang, X.Hu (2011). Study on the precipitation behavior of the drill pipe steel microalloyed with Nb. *Adv. Mater. Res.* 335–336 (September), 63–68. doi:10.4028/www.scientific.net/AMR.335-336.63
- Yan, T. N., Xue, W., and Lu, C. H. (2010). Superiorities of aluminum alloy drilling pipe and its application prospects in deep holes for geological exploration. *Explor. Eng.* 37 (2), 27–29.
- Yi, P., Wen, Y., Liang, J., Hou, B., Sun, J., Gu, Y., et al. (2018). Effects of nanocrystallized layer on the tribological properties of micro-arc oxidation coatings on 2618 aluminum alloy under high temperatures. *Int. J. Adv. Manuf. Technol.* 96 (5–8), 1635–1646. doi:10.1007/s00170-017-0831-y
- Yonggang, L., Fangpo, Li, Xin, Xu, Yang, B., and Lu, C. (2011). Simulation technology in failure analysis of drill pipe. *Procedia Eng.* 12, 236–241. doi:10.1016/j.proeng.2011.05.037
- Zhu, X.-H. (2016). "Failure analysis and solution studies on drill pipe thread gluing at the exit side of horizontal directional drilling," in *Handbook of materials failure analysis with case studies from the oil and gas industry* (Elsevier). doi:10.1016/B978-0-08-100117-2.00004-2
- Zhu, X., Dong, L., and Tong, H. (2013). Failure analysis and solution studies on drill pipe thread gluing at the exit side of horizontal directional drilling. *Eng. Fail. Anal.* 33 (October), 251–264. doi:10.1016/j.engfailanal.2013.05.017

Nomenclature

ADP	Aluminum Drill Pipe (-)	θ	Estimated parameter vector (-)
API	American Petroleum Institute (-)	UCFT	Ultrasonic Cold Forging Technology (-)
BHA	Bottom Hole Assembly (-)	V(x)	Displacement vector (m)
d	Mean grain diameter (μm)	Vp	Interfacial surface energy (J/m^2)
D	Outer diameter of drill pipe (m)	Vrs	Resultant speed (m/s)
d_i	Inner diameter of drill pipe (m)	Vts	Tripping speed (m/s)
EI	Flexural stiffness of drill pipe ($\text{N}\cdot\text{m}^2$)	Wz	Section modulus (flexural factor) (m^3)
E	Young's modulus of elasticity (Pa)	x	Axial coordinate along drill pipe (m)
F_s	Side (normal) force acting on drill pipe (N)	y, z	Lateral displacement coordinates (m)
FFD	Free Ferrite Depth (mm)	η	Efficiency -)
FEA	Finite Element Analysis (-)	μ	Coefficient of friction (-)
FEM	Finite Element Model (-)	ω	Angular velocity (rad/s)
f	Clearance between drill pipe and borehole (m)		
g	Acceleration due to gravity (m/s^2)		
GLRT	Generalized Likelihood Ratio Test (-)		
G	Shear modulus (Modulus of rigidity) (Pa)		
HDD	Horizontal Directional Drilling (-)		
HSLA	High Strength Low Alloy steel (-)		
I(x)	Area moment of inertia at position x ($\text{kg}\cdot\text{m}^2$)		
k	Speed constant (-)		
k_y	Hall-Petch constant (Petch gradient) $\text{MPa}\cdot(\mu\text{m})^{1/2}$)		
LEFM	Linear Elastic Fracture Mechanics (-)		
LCF	Low Cycle Fatigue (-)		
MAD	Maximum Affected Depth (mm)		
MAO	Micro-Arc Oxidation (-)		
m	Mass flow rate of drilling fluid (kg/s)		
M	Applied torque ($\text{N}\cdot\text{m}$)		
M_y, M_z	Bending moments about y and z-axes ($\text{N}\cdot\text{m}$)		
N	Number of fatigue cycles to failure (-)		
n	Number of load cycles (-)		
O₂	Second-order zero matrix (-)		
P	Axial force (N)		
PDD	Partial Decarburization Depth (mm)		
Q	Transverse pressure on drill pipe (Pa)		
R	Radius of drill pipe (m)		
ROP	Rate of Penetration (m/h)		
SEM	Scanning Electron Microscopy (-)		
S-N	Stress-life fatigue approach (-)		
S_m	Mean stress (MPa)		
S_r	Stress range (MPa)		
σ	Yield strength (MPa)		
σ_c	Critical crack propagation stress (MPa)		